

Article

A Coaxial Dielectric Barrier Discharge Reactor for Treatment of Winter Wheat Seeds

Thalita M. C. Nishime ^{*}, Nicola Wannicke, Stefan Horn, Klaus-Dieter Weltmann  and Henrike Brust ^{*}

Leibniz Institute for Plasma Science and Technology (INP), D-17489 Greifswald, Germany; nicola.wannicke@inp-greifswald.de (N.W.); stefan.horn@inp-greifswald.de (S.H.); weltmann@inp-greifswald.de (K.-D.W.)

^{*} Correspondence: thalita.nishime@inp-greifswald.de (T.M.C.N.); henrike.brust@inp-greifswald.de (H.B.)

Received: 10 September 2020; Accepted: 10 October 2020; Published: 13 October 2020



Abstract: Non-thermal atmospheric pressure plasmas have been recently explored for their potential usage in agricultural applications as an interesting alternative solution for a potential increase in food production with a minor impact on the ecosystem. However, the adjustment and optimization of plasma sources for agricultural applications in general is an important study that is commonly overlooked. Thus, in the present work, a dielectric barrier discharge (DBD) reactor with coaxial geometry designed for the direct treatment of seeds is presented and investigated. To ensure reproducible and homogeneous treatment results, the reactor mechanically shakes the seeds during treatment, and ambient air is admixed while the discharge runs. The DBD, operating with argon and helium, produces two different chemically active states of the system for seed modification. The temperature evolution was monitored to guarantee a safe manipulation of seeds, whereas a physiological temperature was assured by controlling the exposure time. Both treatments led to a remarkable increase in wettability and acceleration in germination. The present study showed faster germination acceleration (60% faster after 24 h) and a lower water contact angle (WCA) (82% reduction) for winter wheat seeds by using the described argon discharge (with air impurities). Furthermore, the treatment can be easily optimized by adjusting the electrical parameters.

Keywords: plasma agriculture; DBD; wheat; germination acceleration; seed; cold atmospheric plasma (CAP); plasma source

1. Introduction

Wheat has been cultivated for about 10,000 years, and it is used in various cultures as a staple food and livestock feed [1]. It is considered to be one of the most important cereal crops worldwide with great adaptability for growing conditions and huge flexibility for food varieties. Moreover, it can be effectively stored for an undefined period if kept dry and if pests are controlled. Wheat has an annual harvest over 700 million tonnes, where the European Union is the largest producer, followed by China and India [2]. However, the estimated production could fall below 2019's level according to the Food and Agriculture Organization of the United Nations (FAO) [2], due to drought weather conditions in the EU in 2020. With climate change and a continuously increasing world population with raising demand for food, problems with production rate might become more frequent. In addition, problems in chemical pests control regarding insect biodiversity and an increased loss of licensed agrochemicals occur. Thus, besides the traditional methods with conventional breeding and the use of agrochemicals, the search and development of new and efficient non-chemical techniques for improving plant growth and resistance against plant diseases and abiotic stresses have evolved to be

an urgent topic. Among them, the use of plasma in agriculture has gained increasing attention over time [3–6].

Non-thermal atmospheric pressure plasmas offer unique possibilities for the treatment of heat-sensitive targets, such as polymers and biological organisms [7,8]. In the last decade, the number of published papers dealing with its use in agriculture has linearly risen [9]. In this field, scientists have observed that plasmas are able to sanitize food products and decontaminate plant seeds, fruits, and vegetables [5,10–12]. Several authors have reported the efficient improvement of the germination and growth of agriculturally relevant plant species such as wheat [13–24], maize [14,25], lupine [14], soya beans [26,27], mung beans [28], radish [29–31], pea [32–35], and rice [29,36]. It has been shown that exposure to plasma improves water uptake by the seed [34,37], decreases the contact angle of the seed surface [23,37], and functionalizes the seed coat by attaching new chemical bonds to the surface [34,38]. In addition to physical changes at the seed surface, physiological alterations along with effects on seedling growth and development [39,40] and improved tolerance against various stresses [11,41] have been observed as well. However, depending on the plasma source and treatment conditions, negative effects on germination and seedling growth are observed [39,42]. Thus, the type of treatment (direct or indirect), reactor configuration, gas, and electrical parameters have an impact on the germination and further plant growth [42]. Moreover, the reactor geometry needs to be adapted according to the target type and application desired. Cold plasmas can be generated at atmospheric pressure using different reactor configurations [43]. Among them, plasma jets provide only a small plasma plume for surface treatment, which considerably limits the active zone [44]. Corona discharge reactors can easily be up-scaled to increase the treatment area by implementing several additional electrodes [45]. The discharge produced is quite inhomogeneous and can affect the substrate non-uniformly. Dielectric barrier discharge (DBD) reactors present great flexibility concerning the electrode's arrangement [46] due to their coplanar configuration allowing the indirect treatment of substrates until planar and coaxial configurations, producing big volumes of plasma. Depending on the feeding gas and construction, DBDs can provide rather homogenous treatments. Therefore, they can be the most suitable choice for the direct treatment of seeds (seeds in direct contact with the discharge).

DBDs are widely reported in scientific papers for the treatment of seeds and plants. Due to their simple and flexible construction, DBDs can be easily adapted for the treatment of different types of substrates. Table 1 summarizes a variety of volume DBD reactors and the corresponding parameters used for the treatment of seeds in the past 5 years. The majority of used DBD reactors are with planar configuration (parallel plates) operating at atmospheric pressure. Half of the listed studies (12) operate the discharge in air. To avoid high voltages because of the breakdown voltage necessary to ignite the plasma in such conditions, either the gap needs to be reduced (diminishing the amount of seeds that can fit inside) or the pressure of the gas has to be lowered. Another aspect is the application of additional rotating or vibrating mechanical parts into the system to ensure a homogeneous treatment of all seeds. Butscher and coauthors [47] assembled the parallel plates reactor on a horizontal vibrating table. Piza and coauthors [48] mechanically moved the seeds during treatment. The planar reactor used by Billah and coauthors [49] had a rotating system that provided seeds motion, and Magureanu and coauthors [50] made use of a strong gas flow rate (15 slm) inside the reactor with coaxial configuration.

Table 1. Literature overview of dielectric barrier discharge (DBD) reactors used for seed treatment in the last 5 years.

Geometry	Movement System	Volume **	Gap	Gas	Pressure	Electrical Parameters		Gas Temp.	Plant Species	Treatment Time	Ref.
						Frequency	Power and Voltage				
Planar	No	≈28.5 cm ³	3 mm	Ar (1–2 slm)	1 atm	13 kHz	0.84 W/cm ²	<30 °C	Chicory seeds	60 and 120s	[51]
							0.84 W/cm ² and 10 kV		<i>Catharanthus roseus</i>	15, 30, 60 and 90 s	[40]
							0.84 W/cm ²		Wheat seeds	15, 30, 60, 90, and 120 s	[13]
							0.84 W/cm ² and 11 kV		Pepper seeds	60 and 120 s	[52]
						N.I.	0.84 W/cm ²		<i>Salvia nemorosa</i> L.	80 and 100 s	[53]
Planar	Yes	20 cm ³	10 mm	He (10 slm)	1 atm	35 kHz	15 kV	Room temp.	Hybrid corn	10 s	[54]
Planar	Yes	≈95.4 cm ³	60 mm	Air	≈0.5 atm *	4.5 kHz	45 W and 5 kV	~37 °C	Black gram seeds	20, 40, 60, 90, 120, 180 s	[49]
Planar	Yes	100 cm ³	5 mm	Ar (5.6 slm)	1 atm	2.5–10 kHz (pulsed)	6–10 kV	<100 °C	Onion, radish, cress and alfalfa seeds	2–10 min	[47]
Planar	No	5300 cm ³	20 mm	Air	≈0.002 atm *	5.28 Mhz	0.025 W/cm ³	<37 °C	Maize, Lupine and Winter wheat seeds	2, 4, 5 and 7 min	[55]
Planar	No	≈21.1 cm ³	4.2 mm	Air	≈0.5 atm *	1 kHz	6.4 W and 8.2 kV	<25.5 °C	Quinoa seeds	10, 30, 60, 180, and 900 s	[38]
Planar	No	≈62.8 cm ³	8 mm	Air (1.5 slm)	1 atm	50 Hz	9–17 kV	Room temp.	Wheat seeds	4 min	[21]
							13 kV			4 min	[41]
							1.5 W and 13 kV			1, 4, 7, 10, and 13 min	[22]
				O ₂ , air, Ar, N ₂ (1.5 slm)			13kV			4 min	[20]
Planar	No	≈78.5 cm ³	10 mm	He (2 slm) + 0.5% O ₂	1 atm	10 kHz	30 W	N.I.	Grape seeds	2, 5 and 10 min	[56]
				He (2 slm)			50 W	10 °C above room temp.	Grape and coffee seeds	30, 60, 120, and 240 s	[57]

Table 1. Cont.

Geometry	Movement System	Volume **	Gap	Gas	Pressure	Electrical Parameters		Gas Temp.	Plant Species	Treatment Time	Ref.
						Frequency	Power and Voltage				
Planar needle array	Yes	≈113.1 cm ³	10 mm	O ₂ and N ₂ (6 slm)	1 atm	50 Hz	65 W or 85 W	Room temperature	Soybean seeds	1, 2, and 3 min	[48]
Planar	No	≈19.6 cm ³	10 mm	Air	1 atm	50 Hz	10 kV	<40.2 °C	Wheat seeds	3 min	[58]
Planar	No	6 cm ³	10 mm	Air (1 slm)	1 atm	200 Hz (pulsed)	130 W/cm ³ and 21 kV	Room temp.	Radish, tomato and sweet pepper seeds	10 and 20 min	[59]
Planar	Yes	≈4 cm ³	<4 mm	Air	1 atm	22.5 kHz	30 W and 10 kV	<40 °C	Wheat seeds	2–10 s	[60]
Planar	No	≈19.1 cm ³	12 mm	He (5 slm)	1 atm	16 kHz	30 W and 20 kV	N.I.	Wheat seeds	10–900 s	[24]
Planar	No	≈141.4 cm ³	8 mm	Air	1 atm	N.I.	9–35 W	N.I.	Pea seeds	1, 3, 5, 7, and 10 min	[34]
Coaxial	No	N.I.	N.I.	N.I.	1 atm	990 Hz (pulsed)	1.8 mW/cm ² and 35 kV	N.I.	<i>Mimosa caesalpiniaefolia</i>	3, 9, and 15 min	[61]
Coaxial	Yes	N.I.	4 mm	Air (15 slm)	1 atm	50 Hz	0.55; 1.01 and 1.43 W/13; 15 and 17 kV	Room temp.	Tomato seeds	13 min (13 kV)–7 min (15 kV)–5, 30, and 45 min (17 kV)	[50]

* Converted values; ** calculated values; N.I.: not informed data; temp.: abbreviation for temperature.

In the present work, a cylindrical DBD reactor intended for the direct treatment of seeds is presented. The reactor is mounted on top of a vortex mixer device that allows the seeds to shake during the process, ensuring homogeneous treatment. The reactor, with a volume of around 88 cm³, allows the easy introduction of different feed gases and can be easily scaled up, which makes it suitable as a prototype for laboratory tests and optimization. In this study, the efficiency of treating winter wheat seeds has been compared by operating the reactor with two feed gases (argon and helium) with same gas flow rate and same discharge power. The results show that even though both discharges present similar excited reactive species (N₂, OH, and NO), the argon plasma leads to a further reduction of the water contact angle (WCA) measured at the seed coat of wheat seeds. In contrast, the seeds exposed to the helium plasma present stable WCA values for longer treatment times. Additionally, the argon treatment leads to a much more pronounced germination acceleration compared to the helium plasma. In addition, it has been shown that varying the electrical parameters can drastically reduce the treatment time.

2. Materials and Methods

2.1. Plasma Source

The plasma source used in this study consists of a laboratory scale dielectric barrier discharge (DBD) reactor with coaxial configuration. It comprises of a borosilicate glass tube with one closed end mounted on top of a vortex mixer, as shown in Figure 1. Around the glass tube (length of 10 cm, outer diameter of 40 mm, and glass thickness of 2.3 mm), a wrapped copper tape in spiral shape is connected to high voltage, while in its central axis, a copper rod crossing the entire length serves as the grounded electrode, forming a gap distance of 13 mm. Details of the electrode's arrangement can be seen in the cross-section cut (A-A) in Figure 1. The reactor is closed by a plastic cap that allows gas introduction. Some holes in the cap next to the gas entrance connection help control the pressure rise inside the reactor and serve as a gas outlet.

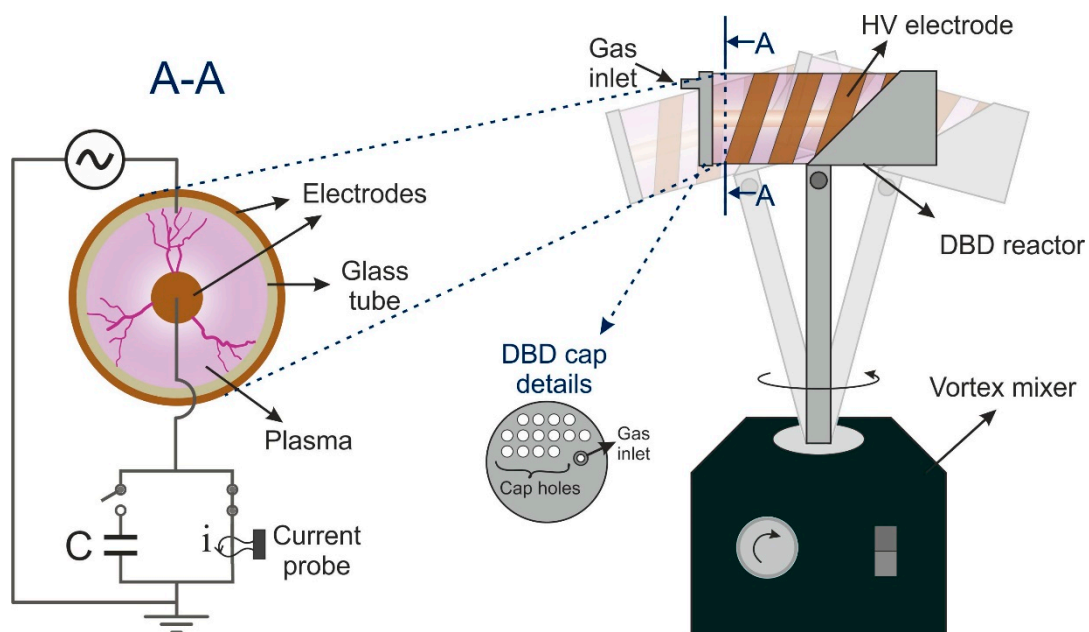


Figure 1. Experimental setup of the coaxial DBD reactor used for seed treatment.

The DBD was operated with an alternating current (AC) power supply with a frequency of 10 kHz and adjustable applied voltage. The sinusoidal voltage signal was amplitude modulated using burst mode, which helps reduce the discharge temperature. In this work, the voltage duty cycle was kept at 30% with a repetition frequency of 10 Hz for all experiments. In Section 3.5, the duty cycle was

varied, but repetition frequency was kept constant. In order to assess its effectivity to seed treatment, the reactor was fed with two different gases, argon and helium, at a flow rate of 2.0 slm.

2.2. Electrical Characterization

For the electrical characterization of the coaxial DBD, the charge and current transferred to the grounded electrode were measured as schematized in Figure 1. A current probe (TEK CT-2, Tektronix, Beaverton, OR, USA) was connected around the grounding cable to measure the discharge current. Alternatively, the reactor was grounded through a 1.0 nF mica capacitor for measuring the transferred charge. Applied voltage and voltage drop at the capacitor were obtained through a voltage divider (1000:1) at the high voltage electrode and across the capacitor, respectively. The signals were monitored using a digital oscilloscope (Waverunner 8254M 2.5 GHz, Lecroy, Chestnut Ridge, NY, USA). The discharge power was determined using the Q-V Lissajous figure method [62] to obtain the discharge energy per one cycle of applied voltage.

2.3. Optical Emission Spectroscopy (OES)

The excited species in the discharge were identified by optical emission spectroscopy (OES) in the wavelength range between 200 and 960 nm. A set of collimating quartz lenses was employed to focus the light beam from the discharge through one cap hole into the optical fiber connected to the dual-channel spectrometer (AvaSpec-2048-2-USB2, Avantes, Apeldoorn, The Netherlands). The spectrometer has a spectral resolution of around 0.7 nm.

2.4. Temperature Measurements

For the discharge temperature, a non-conductive GaAs-based fiber optic temperature sensor (TS2, OPTOcon, Weidmann Technologies Deutschland GMBH, Dresden, Germany with a diameter of 200 μm connected to a fiber optic temperature measurement device (FOTEMP1-OEM, OPTOcon) was used. This sensor provides a voltage signal output proportional to the temperature. The fiber was inserted inside the reactor through one of the cap holes and kept fixed in the middle of the discharge tube where the gas temperature was acquired for 10 min with plasma on. Subsequently, plasma was turned off, and the temperature drop was measured for 5 min.

Immediately after the plasma treatment of seeds, the temperature at the seed coat was measured using an infrared (IR) thermal camera (FLIR E50, FLIR, Wilsonville, OR, USA). For the IR pictures, the seeds were placed on top of a wooden surface to reduce reflection interferences.

2.5. Plasma Treatment of Wheat Seeds

Winter wheat seeds (variety reform and seed moisture around 12%) obtained from Ceravis AG (Rendsburg, Germany) were treated with plasma using the coaxial DBD working with two different gases: argon and helium. First, 15 cm^3 of seeds were filled inside the reactor for each treatment condition. All treatments were performed with the vortex mixer at medium speed, allowing a constant mixing of the seeds. To ensure treatment reproducibility, the reactor was always operated with the same amount of seeds, and the shaking speed was kept constant for all treatments. The air humidity was kept constant at around 30%. The maximum treatment time was set to 5 min due to an increase in temperature. Thus, the seeds were treated from 3 to 30 min where, for long treatment times (above 5 min), breaks of 5 min in between treatments were taken. Two control groups were considered here: the control (c) with untreated seeds and the gas control (c_g), where seeds were placed inside the reactor for 5 min with the gas and the vortex mixer on.

2.6. Water Contact Angle (WCA) Analysis

Water contact angle (WCA) measurements using the sessile drop method were performed after plasma treatment using a goniometer OCA 30 (DataPhysics Instruments, Filderstadt, Germany).

The wheat seeds were glued on top of a flat surface with the crease facing down. A drop of 2.0 μL of deionized water was placed on top of its convex side, and the evaluation was carried out with the software SCA 20 (DataPhysics Instruments). For each treatment parameter, a set of 10 seeds was analyzed.

2.7. Germination Tests

The germination tests were carried out in $12 \times 12 \text{ cm}^2$ square Petri dishes with 4 layers of absorbent paper. Germination experiments were initiated immediately after plasma treatment. For each parameter, 4 replicates with 50 seeds each were analyzed. The seeds were evenly distributed on top of the paper layers that were humidified with 10 mL of water. The germination process took place inside a dark chamber with a controlled temperature of 22 $^\circ\text{C}$ and was monitored from 9 h (argon) and 15 h (helium) after placing the Petri dishes inside the chamber until the germination reached its maximum value. Seeds were considered germinated when the emerged radicle reached at least 1 mm. The germination percentage (Gp) was calculated according to Equation (1) [63]:

$$Gp(\%) = \frac{N_i}{N} 100 \quad (1)$$

where N_i corresponds to the number of germinated seeds at a given time interval, and N corresponds to the total number of seeds in the Petri dish.

2.8. Statistical Analysis

All statistical analyses were done using SigmaPlot 13 (SigmaPlot, San Jose, CA, USA). Germination data were analyzed by two-way ANOVA applying the following fixed factors: (a) type of treatment (exposure time, duty cycle) and the time interval of germination (15 h, 18 h, 21 h, 24 h, 40 h, and 48 h) and (b) working gas (argon and helium) and treatment (from 3 to 30 min). If significant differences occurred, a post hoc test (Holm–Sidak method) was used to identify individual treatments with significant deviations.

3. Results and Discussion

3.1. Discharge Characterization of the DBD Reactor Operating with Different Feed Gases

The coaxial DBD reactor was fed with two different gases: argon and helium. Figure 2 presents the electrical signals of both discharges operating with a duty cycle of 30% and amplitude voltage of 6 kV. In both graphs, current peaks can be observed during the rising and falling parts of the voltage. Argon plasmas are generally filamentary; i.e., they are constituted by several short-lived discharge filaments randomly distributed over the entire electrode's surface [46]. This filamentary characteristic of argon plasmas is evidenced by the multiple current peaks in both the positive and negative half-cycle of the voltage in Figure 2a. It can also be observed in the discharge picture presented along with the current waveform in Figure 2c. On the other hand, helium plasmas can operate in glow mode at atmospheric pressure, and their current waveform is characterized by one single peak in the positive and one in the negative half-cycle of the voltage [64]. Figure 2b exhibits the current and voltage waveforms for the helium discharge using the shaking DBD reactor. Here, several current peaks can be observed even though the discharge is clearly homogeneous, as to be seen in Figure 2d. The electrical signals presented in Figure 2a,b were acquired with seeds placed inside the reactor, while the formation of several current peaks in the helium DBD can be associated to a possible charge density enhancement caused by the accumulation of charge at the seeds surface [65]. The formation of several current peaks in a helium discharge can also be related to the presence of N_2 impurities, as investigated by Martens and coauthors [66]. Thus, the formation of the current peaks observed in Figure 2b can also be attributed to the high level of impurities inside the reactor caused by the vortex mixer device leading to an admixture of ambient air into the discharge region.

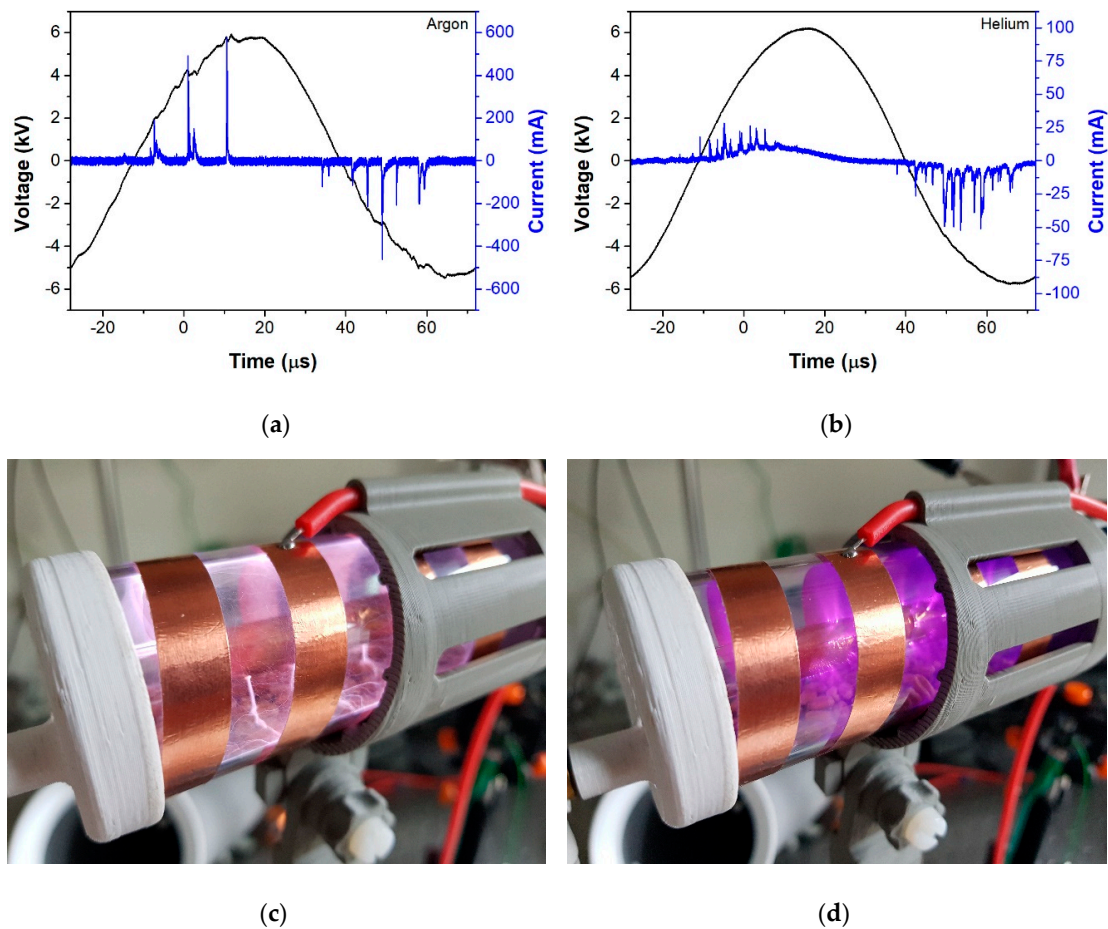


Figure 2. Current and voltage waveforms of the discharges generated in (a) argon and (b) helium along with pictures of the discharges in (c) argon and (d) helium.

The formation of several short-lived current peaks can complicate the assessment of the dissipated power in the discharge by current integration. Therefore, the discharge power was evaluated by the QV Lissajous figure method. Figure 3 presents the power values for different applied voltages for both discharges (argon and helium). It can be observed for both cases that the power values tend to rise almost linearly with the increase of applied voltage, where the argon plasma (black curve) exhibits higher power values than the helium (red curve). For a voltage range between 10 and 14.5 kV peak to peak (p-p), the power values can vary from 1 to 10 W, which also leads to a temperature rise that could harm the seeds. In order to compare both discharges, different parameters were chosen for both gases operating with around 6.5 W of mean power (73.9 mW/cm^3), resulting in an applied voltage of 11.5 kV p-p for argon and 13 kV p-p for helium.

Varying the feed gas can modify the produced plasma excited species, and thus, optical emission spectroscopy (OES) was used to analyze both discharges during wheat seed treatment. Figure 4 presents the optical emission spectra of argon (a) and helium (b). One important common feature between the two spectra is the presence of weak $\text{NO}(\gamma)$ emission below 280 nm with similar intensity. Emission bands of OH (308 nm) and an N_2 second positive system (between 300 and 500 nm) can also be observed for both spectra due to the slots at the reactor cap allowing an admixture of ambient air. The argon discharge emission spectrum (Figure 4a) presents strong Ar atomic lines between 650 and 900 nm and an intensive OH peak when compared to the weak nitrogen emission bands. It is important to notice the preferred energy transfer to oxygen species rather than N_2 in the argon plasma evidenced by the hydroxyl radical peak and weak atomic oxygen line in 777 nm and less intense N_2 peaks.

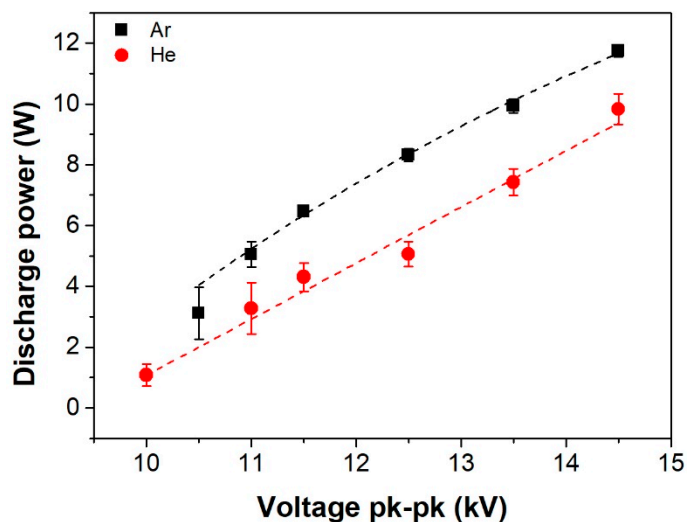


Figure 3. Dependence of the discharge power on applied voltage for argon (black) and helium (red).

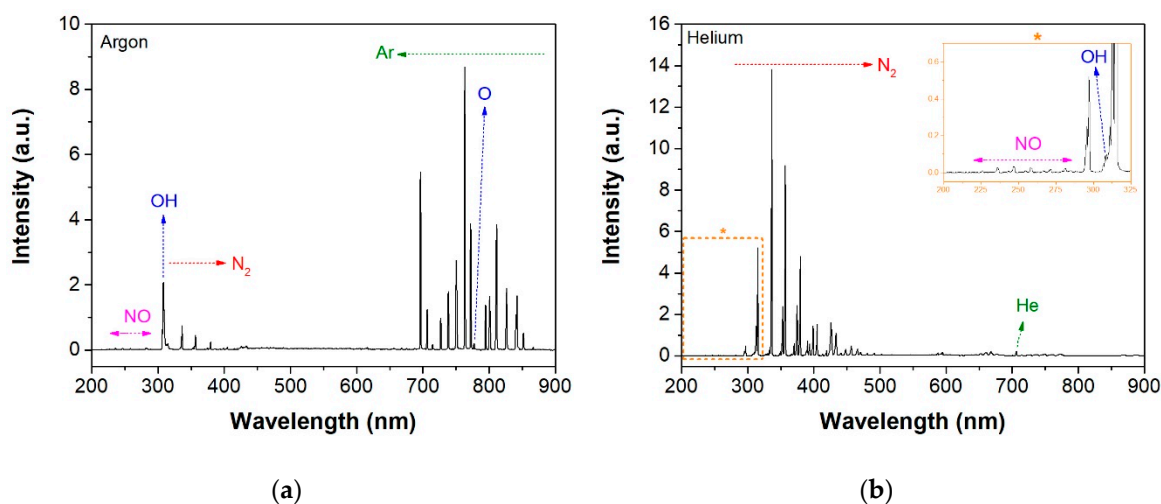


Figure 4. Optical emission spectra of the discharges generated in (a) argon and (b) helium.

The emission spectrum of the helium discharge presented in Figure 4b exhibits very intensive bands of nitrogen (second positive system). The OH band at 308 nm originated from ambient moisture is very weak in comparison with the argon discharge spectrum (Figure 4a). Only a weak atomic He line can be observed at 706 nm. The low-intensity He line in Figure 4b confirms the efficient energy transfer from helium metastable species to nitrogen molecules prioritizing the formation of reactive nitrogen species (RNS) [67]. This shaking DBD reactor acts as an open system allowing ambient air to permeate the discharge region. Hence, reactive oxygen and nitrogen species (RONS) are produced in the discharge after admixture inside the reactor [68]. According to Figure 4a,b, different intensity levels of excited oxygen and nitrogen were observed for each feed gas, suggesting that, on one hand, the argon plasma might generate more reactive oxygen species (ROS) than reactive nitrogen species. While, on the other hand, the higher intense peaks of excited nitrogen in the helium plasma (Figure 4b) indicates the opposite (the biggest production of RNS when compared to ROS). Thus, both discharges provide different chemically active states of the system, which might impact the seeds in distinct ways. The percentage of air and the concentration of produced reactive species are important parameters to be considered when upscaling the reactor for agricultural applications. In such a case, the exact amount of air admixture should be previously determined to ensure results reproducibility. Thus, such open questions (reactive species production according to different percentages of air admixture) will be discussed and answered in future work.

3.2. Impact of the DBD Reactor Operation Time on the Temperature Evolution

Figure 5a presents the curves of temperature increase during 10 min of plasma on for argon (black curve) and helium (red curve) with a discharge power of 6.5 W. Both curves rapidly increase with time clearly tending to saturation, where the helium discharge temperature rises to about 5 °C more than for the argon. This difference might be explained by the higher thermal conductivity of helium heating up the entire discharge volume more homogeneously, while for the argon plasma, the biggest temperature gradient occurs in the filaments (Figure 2c), leading to an average lower temperature value. Running the plasma source for up to 10 min led to an increase of temperature to around 55 and 60 °C for argon and helium, respectively. Thus, in order to avoid the overheating of biological targets, a limitation of 5 min of maximum treatment time was established for such discharge parameters. Switching off both discharges (Figure 4a) after 10 min of plasma on causes the temperature to drop, reaching physiological temperatures after 5 min. Therefore, for seed treatments longer than 5 min using this coaxial DBD, a minimum 5-min pause in between treatments was taken.

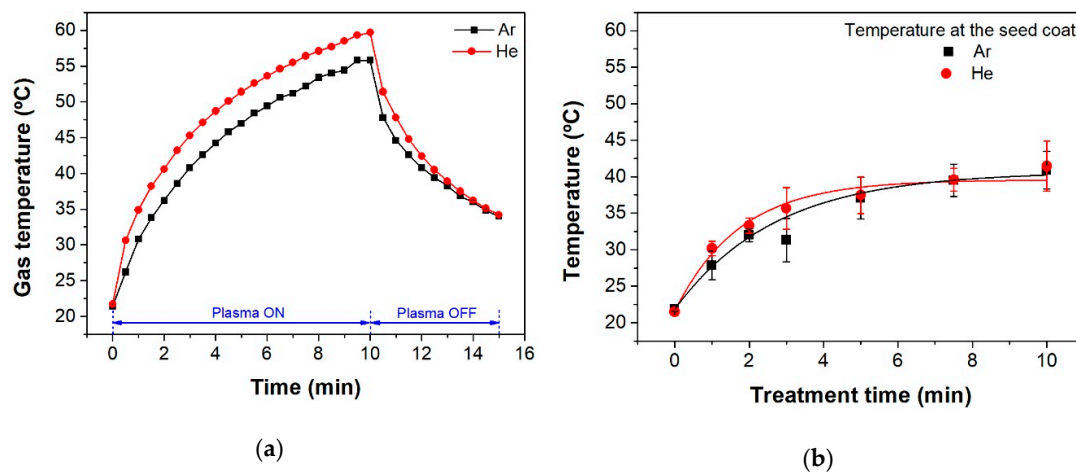


Figure 5. Temperature measured (a) inside the reactor for both gases during 10 min of plasma on and cooling process after plasma is turned off. (b) Temperature at the seed coat of wheat treated for treatment times varying from 1 to 10 min using an argon (black) and helium (red) discharge.

Winter wheat seeds were exposed to both plasmas (argon and helium) in order to check the temperature evolution at the seed coat. The seed's temperature was measured using an IR camera directly after plasma treatment for different exposure times. The curves are shown in Figure 5b where the same trend for the gas temperature can be observed. However, the temperature values at the seed coat tend to saturate at shorter treatment times, remaining below 41 °C. The seed's temperature is comparable when wheat is treated with both gases, reaching around 37 °C after 5 min of plasma treatment. Therefore, no heat damage caused by the plasma is expected when keeping 5 min as the maximum treatment time using 30% of voltage duty cycle and a discharge power of around 6.5 W.

3.3. Effects on Seed Surface Wettability of Wheat for Both Discharges

Water contact angle (WCA) measurements can be used to evaluate surface wettability, which can be modified due to chemical and physical alterations caused by plasma treatment [69]. For the untreated wheat seed surface analyzed here, an average contact angle of around 110° was obtained. Even considering seeds from different origins (e.g., variety, country, harvest year, company), this value is in good agreement with other published studies about wheat seeds such as 113° observed by Velichko and coauthors [60], 106° from Los and coauthors [70], and 120° measured by Molina and coauthors [24]. Figure 6 presents the WCA measurements of untreated seeds (control) and seeds treated from 1 to 30 min with argon (black curve) and helium (red curve). A steep WCA reduction can be observed already for only 1 min treatment in both cases, where the contact angles are reduced

from 110° to around 45° and 55° when treated with argon and helium, respectively. Increasing the treatment time led to further WCA reduction in the case of the argon discharge resulting in angles about 82% smaller than the control. Meanwhile, the WCA of seeds treated with the helium discharge was not further altered, reaching saturation around 40° with 5 min of treatment time (reduction of around 64%). WCA reduction on the seed coat of wheat seeds treated with DBDs were also observed in other studies, where Molina and coauthors [24] obtained a reduction of around 88% after 15 min of He plasma exposure, and Los and coauthors [70] observed a decrease of only 18% of WCA after 3 min of plasma treatment in open air.

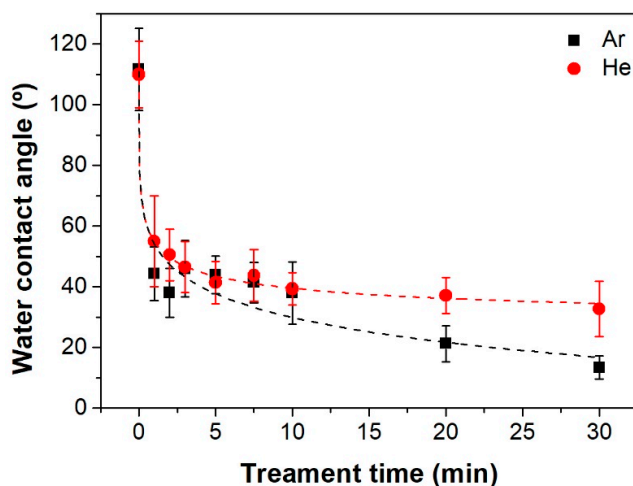


Figure 6. Water contact angle of wheat seeds treated for different treatment times from 1 to 30 min using an argon (black curve) and helium (red curve) discharge. Gas control values for both gases are in the same range as the control points: argon control is $107^\circ \pm 12^\circ$ and helium control is $111^\circ \pm 9^\circ$. Curves were fitted with a logistic function.

Exposing seeds to plasma-generated reactive species can cause modifications on the seed coat, resulting in improved wettability. Thus, the higher reduction of WCA obtained here for the argon-treated seeds might be associated to a bigger amount of oxygen groups attached to the seed, forming polar groups. The increase in the wettability of treated seeds has been reported in the literature also for different types of plasma sources and plant species, where it is commonly related to improvements in water uptake by the seeds, which leads to enhanced seed germination [45,71].

3.4. Effects on Seed Germination of Wheat Treated with Argon and Helium Plasmas

Germination tests were performed with control groups (untreated seeds and seeds subjected to gas only) and plasma-treated seeds for different exposure times (Figure 7). Plant seed germination showed a typical course of germination speed: a lag phase within 24 h (time of imbibition and activation of metabolisms and physiological processes) followed by a log phase where germination speed rises (measured macroscopically by the appearance of the radicle), and finally, a slowdown of germination speed by reaching a plateau and the maximum value of germination. Figure 7 presents the germination analyzed for several time intervals for seeds treated with (a) argon and (b) helium. At given germination conditions, untreated wheat started germinating after around 15 h and reached 100% germination after 48 h. No statistical difference (two-way ANOVA) was observed between the control groups within the observation time (15–48 h), indicating that neither the gas nor the shaking movement stimulates germination. It is clear that plasma treatment with argon and helium using the shaking reactor did not harm the seeds even after 30 min of plasma treatment (6 times 5 min of direct exposure), where 100% germination was still achieved. For both gases, an acceleration of germination can be observed already for short treatment times. In case of the argon discharge, germination acceleration is further enhanced with an increase of exposition time, in which an increase from 11% for 3 min plasma treatment to

around 40% for 30 min plasma treatment of germinated wheat seeds was obtained in the first 15 h. Interestingly, for most of the plasma treatments, seed germination was already in the log-phase for the 15 h observation time and started the saturation course at 24 h for all plasma-treated seeds. Moreover, within the log-phase of germination, an enhancement of germination was observed with longer plasma treatment time (e.g., 3 min < 5 min < 15 min < 30 min). The cumulative germination values for all plasma-treated seeds were statistically significant (two-way ANOVA, $p < 0.001$ – 0.05 , $n = 4$) compared to both control groups from 15 to 24 h of observation time, except for 3 min plasma treatment at 15 h of observation time. On the other hand, with the helium plasma treatment, the acceleration of germination was less pronounced compared to the argon case. Thus, only 3.5% enhancement for 3 min helium plasma-treated seeds to 6.5% enhancement for 30 min of helium plasma treatment was observed. Moreover, for the helium discharge case, the germination of wheat seeds was less enhanced with longer exposure times from 3 to 30 min; thus, the seeds were not significantly different from each other during the observation times of germination. Statistically significant differences (two-way ANOVA, $p \leq 0.02$, $n = 4$) between helium-treated seeds for all exposure times and control groups were only observed at 24 h germination time. A decrease of germination speed started beyond 27 h during germination.

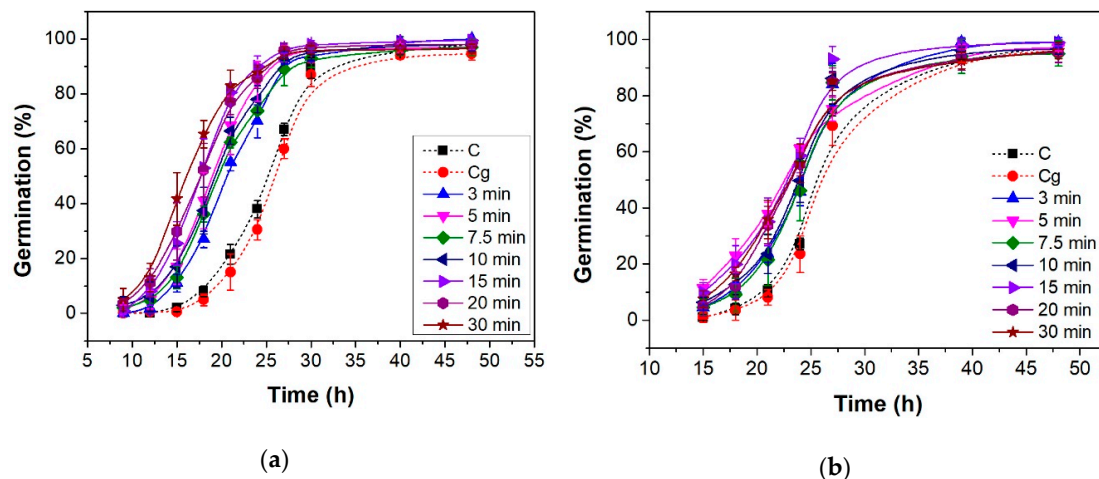


Figure 7. Germination acceleration of wheat seeds treated for different times (from 3 to 30 min) for both discharges (a) argon and (b) helium. Germination curves were fitted with the Hill function.

In comparison to the WCA measurements (Figure 6), similar trends were detected for seeds treated with argon and helium plasma. Those results could indicate that the further enhanced wettability of argon-treated wheat seeds for longer exposure times might be related to the improvement in water uptake and thus early germination. Moreover, the better performance of the argon treatment might be related to the higher intensities of excited oxygen species detected in the OES spectrum (Figure 4a). According to the study performed by Sarinont and coauthors [30], where different feed gases were used in a surface DBD reactor for seed treatment, nitrogen emission and excited species do not play an important role in the growth enhancement of radish, where the best results were obtained for the oxygen emission containing discharges, e.g., air, O_2 and NO (10%) + N_2 . In a study using helium as the feed gas and an open DBD system, X-ray photoelectron spectroscopy (XPS) data indicated a significant input of oxygen to the wheat seed surface, while carbon concentration was decreased [24]. This was associated to the ionization of air molecules in the discharge that interact with the plasma activated surface, leading to oxidation of the pericarp [24].

With regard to the observed trends in WCA measurements, for treatment times below 10 min (Figure 6), argon and helium plasma treatments displayed quite similar wettability effects on the seed coat. In contrast, comparing the germination curves for 3 min (Figure 8a), 5 min (Figure 8b), and 10 min (Figure 8c) treatment times between seeds treated with argon and helium, it is evident that argon

plasma leads to faster germination than the helium discharge, irrespective of similar wettability values. Statistical significance was observed between argon and helium-treated seeds for observation times between 15 and 24 h for 3, 5, and 10 min of plasma exposure. Seed germination was significantly different from the control except for the 15 h observation time for helium-treated seeds (Figure 8a–c). Therefore, other factors besides an increase in surface wettability properties due to the attachment of polar functional groups to the seed surface might be taken into account mainly for the plasma treatment times shorter than 10 min. It is discussed for several plant species that interactions of plasmas reactive species with seeds not only alter seed coat characteristics but could have an impact on the physiology of germinating seeds as well [72]. Reactive species such as hydrogen peroxide and nitric oxide are known to have effects on many developmental processes in plants [73,74]. Hydrogen peroxide has a central role in many signaling processes during the plant life cycle such as the release of dormancy during seed germination [75]. It is also known that external applied hydrogen peroxide stimulates seed germination [76,77]. Thus, if ROS produced in the discharge can be converted by further reactions with water molecules [78], hydrogen peroxide can be formed, be taken up during the imbibition process, and influence metabolic processes in a positive way.

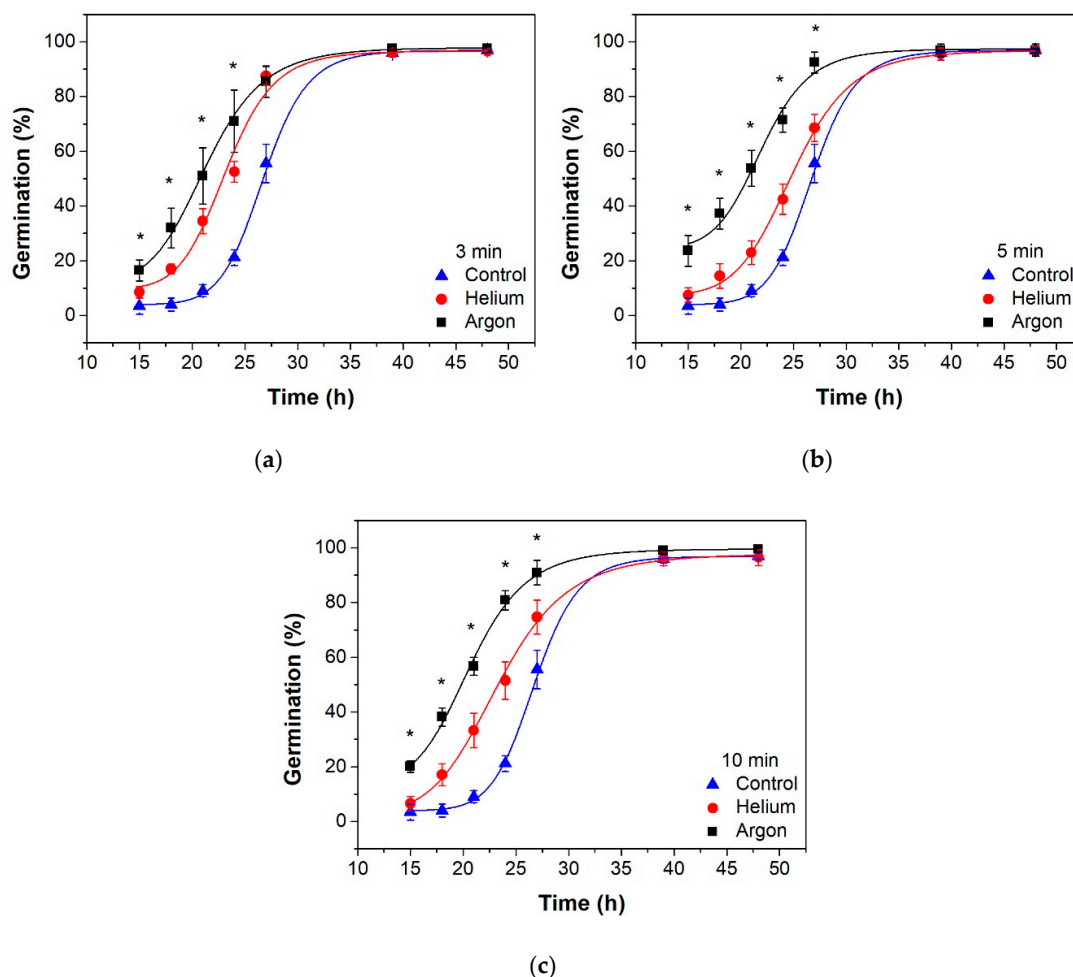


Figure 8. Comparison of germination acceleration of wheat seeds treated with both discharges (argon in black and helium in red) for (a) 3 min, (b) 5 min, and (c) 10 min. Germination curves were fitted with the Hill function. * represents a statistically significant difference ($p \leq 0.001$ – 0.02).

3.5. Variation of Voltage Duty Cycle Affects the Discharge Temperature without Harming the Seeds

The discharge power can be controlled by adjusting the voltage duty cycle. Figure 9a presents the discharge power raise by increasing the duty cycle for the argon discharge, keeping 11.5 kV p-p of

applied voltage. The total dissipated energy per volume unit for the 100% duty cycle (without voltage modulation) was $27.2 \mu\text{J}/\text{cm}^3$ (dissipated power of $25.3 \pm 0.3 \text{ W}$). The previous sections presented measurements with a 30% duty cycle, where the argon discharge was operated at around 6.5 W, and the gas temperature remained around 40 °C. Thus, by varying the voltage duty cycle, the power can be linearly adjusted from 2.5 to 25 W. However, with the increase of discharge power, the gas temperature tends to increase with the same trend. Figure 9b shows the temperature variation after 4 min of plasma on for different voltage duty cycle values where a linear increase of up to 80 °C was obtained for the 90% duty cycle.

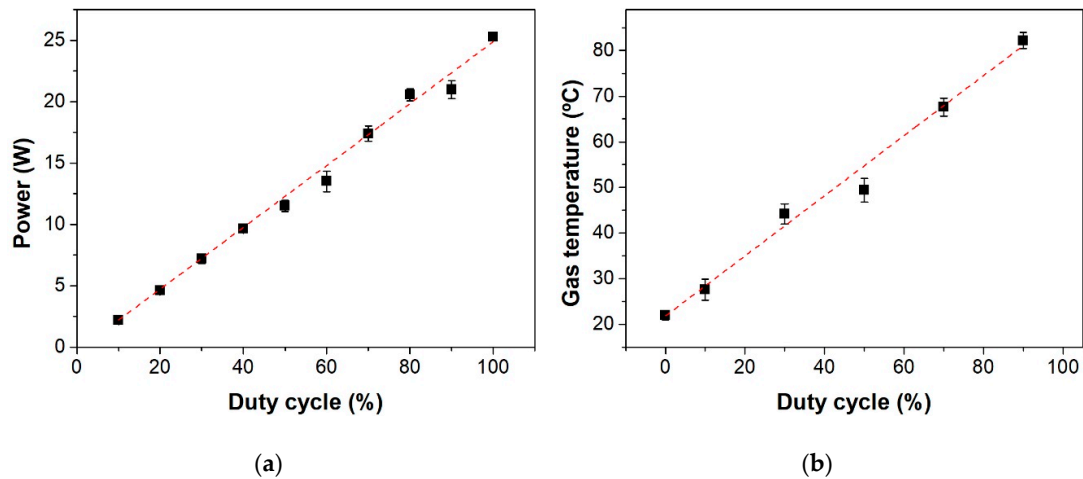


Figure 9. (a) Discharge power increase and (b) linear rise of gas temperature with voltage duty cycle variation for the argon discharge after 4 min from starting the plasma.

Regardless of the higher temperature values achieved, wheat seeds were treated for 4 min with different values of the voltage duty cycle, and the germination test results are presented in Figure 10. It can be clearly seen that even the 90% duty cycle condition that reaches up to 80 °C of gas temperature did not harm the seeds. Moreover, it accelerates the germination as observed for all other tested duty cycle parameters, where the faster germination occurred for the seeds treated with the 50% duty cycle. In this case (for $D = 50\%$), there was a similar acceleration in germination, as the treatment for 30 min with a 30% duty cycle was obtained after only 4 min of plasma exposure. Thus, adjusting the discharge electrical parameters helps optimize the treatment, leading to better results within short time intervals.

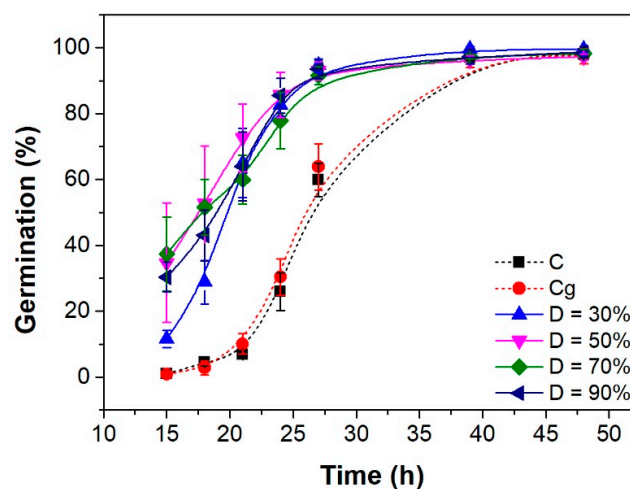


Figure 10. Germination acceleration of argon-treated wheat seeds with different voltage duty cycles for 4 min. Germination curves were fitted with the Hill function.

4. Conclusions

A DBD plasma source operating with argon and helium was investigated for the direct treatment of winter wheat seeds.

The germination speed of wheat seeds could be improved by treating for 3 min with both discharges. Germination effects were stable for treatments up to 30 min. Argon and helium plasmas generated in the shaking DBD reactor produced RONS in different ratios; the argon discharge presented higher excited oxygen emission than nitrogen. Acceleration in the germination of wheat seeds was correlated with the presence of ROS in the discharge, which probably led to the incorporation of oxygen radicals at the seed coat, enhancing water absorption. Thus, the argon discharge treatment led to more pronounced acceleration in germination for long treatment times when compared to control and helium plasma treatment. Similar results were obtained for a shorter treatment time of 4 min by increasing the voltage duty cycle. Thus, the treatment time can be easily reduced by simply adjusting the electrical parameters.

The presented DBD reactor allows accurate control of the discharge power and therefore the gas temperature. The shaking movement allows ambient air to be admixed in the discharge, leading to the generation of RONS. Using the shaking reactor with a set of optimized parameters (e.g., argon with a duty cycle of 50%) led to an improved germination speed that might positively be reflected in later stages of the plant development. The presented DBD reactor can be used to treat plant seeds of variable sizes and shapes, and it can be easily scaled up for agricultural usage and the treatment of a large amount of seeds.

Author Contributions: Conceptualization, T.M.C.N. and H.B.; methodology, T.M.C.N. and H.B.; validation, T.M.C.N., S.H. and N.W.; formal analysis, T.M.C.N., N.W. and H.B.; investigation, T.M.C.N. and S.H.; writing—original draft preparation, T.M.C.N. and H.B.; writing—review and editing, T.M.C.N., N.W., K.-D.W. and H.B.; project administration, H.B.; funding acquisition, K.-D.W., N.W. and H.B. All authors have read and agreed to the published version of the manuscript.

Funding: This research was in parts funded by the Federal Ministry of Education and Research of Germany within the framework of the project “Physics for Food” (BMBF FKZ 03 WIR 2801 B).

Acknowledgments: We are grateful to Robert Wagner and Jasmin Werner for technical assistance during seed germination experiments.

Conflicts of Interest: The authors declare no conflict of interest.

References

1. Shewry, P.R. Darwin review: Wheat. *J. Exp. Bot.* **2009**, *60*, 1537–1553. [PubMed]
2. Food and Agriculture Organization of the United Nations 2018, “Crops”, FAOSTAT. Countries-Select All; Elements-Production Quantity; Items-Wheat; Years-2018. Available online: <http://www.fao.org/faostat/en/#data/QC/> (accessed on 20 June 2020).
3. Brandenburg, R.; Fridman, A.; Reuter, S.; Bogaerts, A.; Bongers, W.; Schiorlin, M.; Verreycken, T.; Ken, K. White paper on the future of plasma science in environment, for gas conversion and agriculture. *Plasma Process. Polym.* **2018**, *16*, 1700238.
4. Bourke, P.; Ziuzina, D.; Boehm, D.; Cullen, P.J.; Keener, K. The Potential of Cold Plasma for Safe and Sustainable Food Production. *Trends Biotechnol.* **2018**, *36*, 615–626. [CrossRef] [PubMed]
5. ŠERÁ, B.; ŠERÝ, M. Non-thermal plasma treatment as a new biotechnology in relation to seeds, dry fruits, and grains. *Plasma Sci. Technol.* **2018**, *20*, 044012.
6. Attri, P.; Ishikawa, K.; Okumura, T.; Koga, K.; Shiratani, M. Plasma Agriculture from Laboratory to Farm: A Review. *Process* **2020**, *8*, 1002. [CrossRef]
7. Šimončicová, J.; Kryštofová, S.; Medvecká, V.; Ďurišová, K.; Kaliňáková, B. Technical applications of plasma treatments: Current state and perspectives. *Appl. Microbiol. Biotechnol.* **2019**, *103*, 5117–5129.
8. Weltmann, K.D.; von Woedtke, T. Plasma medicine—Current state of research and medical application. *Plasma Phys. Control. Fusion* **2016**, *59*, 14031.
9. Ito, M.; Oh, J.-S.; Ohta, T.; Shiratani, M.; Hori, M. Current status and future prospects of agricultural applications using atmospheric-pressure plasma technologies. *Plasma Process. Polym.* **2017**, *15*, 1–15. [CrossRef]

10. Puač, N.; Gherardi, M.; Shiratani, M. Plasma agriculture: A rapidly emerging field. *Plasma Process. Polym.* **2018**, *15*, 1700174.
11. Adhikari, B.; Pangomm, K.; Veerana, M.; Mitra, S.; Park, G. Plant Disease Control by Non-Thermal Atmospheric-Pressure Plasma. *Front. Plant Sci.* **2020**, *11*, 1–15.
12. Mir, S.A.; Shah, M.A.; Mir, M.M. Understanding the Role of Plasma Technology in Food Industry. *Food Bioprocess Technol.* **2016**, *9*, 734–750.
13. Iranbakhsh, A.; Ardebili, N.O.; Ardebili, Z.O.; Shafaati, M.; Ghoranneviss, M. Non-thermal Plasma Induced Expression of Heat Shock Factor A4A and Improved Wheat (*Triticum aestivum* L.) Growth and Resistance Against Salt Stress. *Plasma Chem. Plasma Process.* **2017**, *38*, 29–44. [[CrossRef](#)]
14. Filatova, I.; Azharonok, V.; Lushkevich, V.; Zhukovsky, A.; Gadzhieva, G.; Spasi, K. Plasma seeds treatment as a promising technique for seed germination improvement. In Proceedings of the 31st International Conference on Phenomena in Ionized Gases, Granada, Spain, 14–19 July 2013; pp. 4–7.
15. Scholtz, V.; Sera, B.; Khun, J.; Sery, M.; Julák, J. Effects of Nonthermal Plasma on Wheat Grains and Products. *J. Food Qual.* **2019**, *2019*, 7917825. [[CrossRef](#)]
16. Zahoranová, A.; Henselová, M.; Hudecová, D.; Kaliňáková, B.; Kováčik, D.; Medvecká, V.; Černák, M. Effect of Cold Atmospheric Pressure Plasma on the Wheat Seedlings Vigor and on the Inactivation of Microorganisms on the Seeds Surface. *Plasma Chem. Plasma Process.* **2016**, *36*, 397–414.
17. Roy, N.C.; Hasan, M.M.; Talukder, M.R.; Hossain, M.D.; Chowdhury, A.N. Prospective Applications of Low Frequency Glow Discharge Plasmas on Enhanced Germination, Growth and Yield of Wheat. *Plasma Chem. Plasma Process.* **2018**, *38*, 13–28.
18. Jiang, J.; He, X.; Li, L.; Li, J.; Shao, H.; Xu, Q.; Ye, R.; Dong, Y. Effect of cold plasma treatment on seed germination and growth of wheat. *Plasma Sci. Technol.* **2014**, *16*, 54–58.
19. Sera, B.; Spatenka, P.; Sery, M.; Vrchetova, N.; Hruskova, I. Influence of plasma treatment on wheat and oat germination and early growth. *IEEE Trans. Plasma Sci.* **2010**, *38*, 2963–2968.
20. Meng, Y.; Qu, G.; Wang, T.; Sun, Q.; Liang, D.; Hu, S. Enhancement of Germination and Seedling Growth of Wheat Seed Using Dielectric Barrier Discharge Plasma with Various Gas Sources. *Plasma Chem. Plasma Process.* **2017**, *37*, 1105–1119.
21. Guo, Q.; Meng, Y.; Qu, G.; Wang, T.; Yang, F.; Liang, D.; Hu, S. Improvement of wheat seed vitality by dielectric barrier discharge plasma treatment. *Bioelectromagnetics* **2018**, *39*, 120–131.
22. Li, Y.; Wang, T.; Meng, Y.; Qu, G.; Sun, Q.; Liang, D.; Hu, S. Air Atmospheric Dielectric Barrier Discharge Plasma Induced Germination and Growth Enhancement of Wheat Seed. *Plasma Chem. Plasma Process.* **2017**, *37*, 1621–1634.
23. Los, A.; Ziuzina, D.; Akkermans, S.; Boehm, D.; Cullen, P.J.; Van Impe, J.; Bourke, P. Improving microbiological safety and quality characteristics of wheat and barley by high voltage atmospheric cold plasma closed processing. *Food Res. Int.* **2018**, *106*, 509–521. [[CrossRef](#)] [[PubMed](#)]
24. Molina, R.; Lalueza, A.; López-Santos, C.; Ghobeira, R.; Cools, P.; Morent, R.; de Geyter, N.; González-Eliphe, A.R. Physicochemical surface analysis and germination at different irrigation conditions of DBD plasma-treated wheat seeds. *Plasma Process. Polym.* **2020**, e2000086. [[CrossRef](#)]
25. Henselová, M.; Slováková, L.; Martinka, M.; Zahoranová, A. Growth, anatomy and enzyme activity changes in maize roots induced by treatment of seeds with low-temperature plasma. *Biologia (Bratisl)* **2012**, *67*, 490–497.
26. Ling, L.; Jiafeng, J.; Jiangang, L.; Minchong, S.; Xin, H.; Hanliang, S.; Yuanhua, D. Effects of cold plasma treatment on seed germination and seedling growth of soybean. *Sci. Rep.* **2014**, *4*, 5859. [[CrossRef](#)] [[PubMed](#)]
27. Zhang, J.J.; Jo, J.O.; Huynh, D.L.; Mongre, R.K.; Ghosh, M.; Singh, A.K.; Lee, S.B.; Mok, Y.S.; Hyuk, P.; Jeong, D.K. Growth-inducing effects of argon plasma on soybean sprouts via the regulation of demethylation levels of energy metabolism-related genes. *Sci. Rep.* **2017**, *7*, 1–12.
28. Sadhu, S.; Thirumdas, R.; Deshmukh, R.R.; Annapure, U.S. Influence of cold plasma on the enzymatic activity in germinating mung beans (*Vigna radiate*). *LWT-Food Sci. Technol.* **2017**, *78*, 97–104. [[CrossRef](#)]
29. Shiratani, M.; Sarinont, T.; Amano, T.; Hayashi, N.; Koga, K. Plant Growth Response to Atmospheric Air Plasma Treatments of Seeds of 5 Plant Species. *MRS Adv.* **2016**, *1*, 1265–1269. [[CrossRef](#)]
30. Sarinont, T.; Amano, T.; Attri, P.; Koga, K.; Hayashi, N.; Shiratani, M. Effects of plasma irradiation using various feeding gases on growth of *Raphanus sativus* L. *Arch. Biochem. Biophys.* **2016**, *605*, 129–140. [[CrossRef](#)]

31. Mihai, A.L.; Dobrin, D.; Măgureanu, M.; Popa, M.E. Positive effect of non-thermal plasma treatment on radish seeds. *Rom. Reports Phys.* **2014**, *66*, 1110–1117.
32. Buřler, S.; Herppich, W.B.; Neugart, S.; Schreiner, M.; Ehlbeck, J.; Rohn, S.; Schlüter, O. Impact of cold atmospheric pressure plasma on physiology and flavonol glycoside profile of peas (*Pisum sativum* ‘Salamanca’). *Food Res. Int.* **2015**, *76*, 132–141.
33. Stolárik, T.; Henselová, M.; Martinka, M.; Novák, O.; Zahoranová, A.; Černák, M. Effect of Low-Temperature Plasma on the Structure of Seeds, Growth and Metabolism of Endogenous Phytohormones in Pea (*Pisum sativum* L.). *Plasma Chem. Plasma Process.* **2015**, *35*, 659–676.
34. Gao, X.; Zhang, A.; Héroux, P.; Sand, W.; Sun, Z.; Zhan, J.; Wang, C.; Hao, S.; Li, Z.; Li, Z.; et al. Effect of Dielectric Barrier Discharge Cold Plasma on Pea Seed Growth. *J. Agric. Food Chem.* **2019**, *67*, 10813–10822. [[CrossRef](#)] [[PubMed](#)]
35. Švubová, R.; Kyzek, S.; Medvecká, V.; Slováková, L.; Gálová, E.; Zahoranová, A. Novel insight at the Effect of Cold Atmospheric Pressure Plasma on the Activity of Enzymes Essential for the Germination of Pea (*Pisum sativum* L. cv. Prophet) Seeds. *Plasma Chem. Plasma Process.* **2020**, *40*, 1221–1240.
36. Khamseen, N.; Onwimol, D.; Teerakawanich, N.; Dechanupaprittha, S.; Kanokbannakorn, W.; Hongesombut, K.; Srisonphan, S. Rice (*Oryza sativa* L.) Seed Sterilization and Germination Enhancement via Atmospheric Hybrid Nonthermal Discharge Plasma. *ACS Appl. Mater. Interfaces* **2016**, *8*, 19268–19275. [[PubMed](#)]
37. Zahoranová, A.; Hoppanová, L.; Šimončicová, J.; Tučeková, Z.; Medvecká, V.; Hudecová, D.; Kaliňáková, B.; Kováčik, D.; Černák, M. Effect of Cold Atmospheric Pressure Plasma on Maize Seeds: Enhancement of Seedlings Growth and Surface Microorganisms Inactivation. *Plasma Chem. Plasma Process.* **2018**, *38*, 969–988.
38. Gómez-Ramírez, A.; López-Santos, C.; Cantos, M.; García, J.L.; Molina, R.; Cotrino, J.; Espinós, J.P.; González-Elipe, A.R. Surface chemistry and germination improvement of Quinoa seeds subjected to plasma activation. *Sci. Rep.* **2017**, *7*, 1–12.
39. Cui, D.; Yin, Y.; Wang, J.; Wang, Z.; Ding, H.; Ma, R.; Jiao, Z. Research on the Physio-Biochemical Mechanism of Non-Thermal Plasma-Regulated Seed Germination and Early Seedling Development in Arabidopsis. *Front. Plant Sci.* **2019**, *10*, 1322.
40. Ghasempour, M.; Iranbakhsh, A.; Ebadi, M.; Oraghi Ardebili, Z. Seed priming with cold plasma improved seedling performance, secondary metabolism, and expression of deacetylindoline O-acetyltransferase gene in *Catharanthus roseus*. *Contrib. to Plasma Phys.* **2020**, *60*, e201900159.
41. Guo, Q.; Wang, Y.; Zhang, H.; Qu, G.; Wang, T.; Sun, Q.; Liang, D. Alleviation of adverse effects of drought stress on wheat seed germination using atmospheric dielectric barrier discharge plasma treatment. *Sci. Rep.* **2017**, *7*, 1–14.
42. Sera, B.; Gajdova, I.; Cernák, M.; Gavril, B.; Hnatiuc, E.; Kováčik, D.; Kriha, V.; Sláma, J.; Sery, M.; Spatenka, P. How various plasma sources may affect seed germination and growth. In Proceedings of the 2012 13th International Conference on Optimization of Electrical and Electronic Equipment (OPTIM), Brasov, Romania, 24–26 May 2012; pp. 1365–1370.
43. Tendero, C.; Tixier, C.; Tristant, P.; Desmaison, J.; Leprince, P. Atmospheric pressure plasmas: A review. *Spectrochim. Acta-Part B At. Spectrosc.* **2006**, *61*, 2–30. [[CrossRef](#)]
44. Lu, X.; Naidis, G.V.; Laroussi, M.; Reuter, S.; Graves, D.B.; Ostrikov, K. Reactive species in non-equilibrium atmospheric-pressure plasmas: Generation, transport, and biological effects. *Phys. Rep.* **2016**, *630*, 1–84. [[CrossRef](#)]
45. Bunme, P.; Khamseen, N.; Kasemsuwan, V.; Jitkajornwanich, K.; Pichetjamroen, A.; Teerakawanich, N.; Srisonphan, S. Polarity effect of pulsed corona discharge plasma on seed surface modification. In Proceedings of the 2017 International Electrical Engineering Congress (iEECON), Pattaya, Thailand, 8–10 March 2017.
46. Brandenburg, R. Corrigendum: Dielectric barrier discharges: Progress on plasma sources and on the understanding of regimes and single filaments (2017 Plasma Sources Sci. Technol. 26 053001). *Plasma Sources Sci. Technol.* **2018**, *27*, 079501. [[CrossRef](#)]
47. Butscher, D.; Zimmermann, D.; Schuppler, M.; Rudolf, P.; Rohr, V. Plasma inactivation of bacterial endospores on wheat grains and polymeric model substrates in a dielectric barrier discharge. *Food Control* **2016**, *60*, 636–645. [[CrossRef](#)]

48. Pérez Pizá, M.C.; Prevosto, L.; Zilli, C.; Cejas, E.; Kelly, H.; Balestrasse, K. Effects of non-thermal plasmas on seed-borne Diaporthe/Phomopsis complex and germination parameters of soybean seeds. *Innov. Food Sci. Emerg. Technol.* **2018**, *49*, 82–91.
49. Billah, M.; Sajib, S.A.; Roy, N.C.; Rashid, M.M.; Reza, M.A.; Hasan, M.M.; Talukder, M.R. Effects of DBD air plasma treatment on the enhancement of black gram (*Vigna mungo* L.) seed germination and growth. *Arch. Biochem. Biophys.* **2020**, *681*, 108253. [[CrossRef](#)] [[PubMed](#)]
50. Măgureanu, M.; Sîrbu, R.; Dobrin, D.; Gîdea, M. Stimulation of the Germination and Early Growth of Tomato Seeds by Non-thermal Plasma. *Plasma Chem. Plasma Process.* **2018**, *38*, 989–1001.
51. Abedi, S.; Iranbakhsh, A.; Oraghi Ardebili, Z.; Ebadi, M. Seed priming with cold plasma improved early growth, flowering, and protection of *Cichorium intybus* against selenium nanoparticle. *J. Theor. Appl. Phys.* **2020**, *14*, 113–119.
52. Safari, N.; Iranbakhsh, A.; Ardebili, Z.O. Non-thermal plasma modified growth and differentiation process of *Capsicum annuum* PP805 Godiva in in vitro conditions. *Plasma Sci. and Technol.* **2017**, *19*, 055501. [[CrossRef](#)]
53. Ghaemi, M.; Majd, A.; Iranbakhsh, A. Transcriptional responses following seed priming with cold plasma and electromagnetic field in *Salvia nemorosa* L. *J. Theor. Appl. Phys.* **2020**, 1–6. [[CrossRef](#)]
54. Ahn, C.; Gill, J.; Ruzic, D.N. Growth of Plasma-Treated Corn Seeds under Realistic Conditions. *Sci. Rep.* **2019**, *9*, 1–7. [[CrossRef](#)]
55. Filatova, I.; Lyushkevich, V.; Goncharik, S.; Zhukovsky, A.; Krupenko, N.; Kalatskaja, J. The effect of low-pressure plasma treatment of seeds on the plant resistance to pathogens and crop yields. *J. Phys. D Appl. Phys.* **2020**, *53*, 244001. [[CrossRef](#)]
56. Mujahid, Z.; Tounekti, T.; Khemira, H. Cold plasma treatment to release dormancy and improve growth in grape buds: A promising alternative to natural chilling and rest breaking chemicals. *Sci. Rep.* **2020**, *10*, 1–10.
57. Tounekti, T.; Mujahid, Z.U.I.; Khemira, H. Non-thermal dielectric barrier discharge (DBD) plasma affects germination of coffee and grape seeds. *AIP Conf. Proc.* **2018**, *1976*, 10–14.
58. Rusu, B.G.; Postolache, V.; Cara, I.G.; Pohoata, V.; Mihaila, I.; Topala, I.; Jitareanu, G. Method of fungal wheat seeds disease inhibition using direct exposure to air cold plasma. *Rom. J. Phys.* **2018**, *63*, 1–13.
59. Sivachandiran, L.; Khacef, A. Enhanced seed germination and plant growth by atmospheric pressure cold air plasma: Combined effect of seed and water treatment. *RSC Adv.* **2017**, *7*, 1822–1832.
60. Velichko, I.; Gordeev, I.; Shelemin, A.; Nikitin, D.; Brinar, J.; Pleskunov, P.; Choukourov, A.; Pazderû, K.; Pulkrábek, J. Plasma Jet and Dielectric Barrier Discharge Treatment of Wheat Seeds. *Plasma Chem. Plasma Process.* **2019**, *39*, 913–928. [[CrossRef](#)]
61. Da Silva, A.R.M.; Farias, M.L.; da Silva, D.L.S.; Vitoriano, J.O.; de Sousa, R.C.; Alves-Junior, C. Using atmospheric plasma to increase wettability, imbibition and germination of physically dormant seeds of *Mimosa Caesalpiniaefolia*. *Colloids Surf. B Biointerfaces* **2017**, *157*, 280–285.
62. Holub, M. On the measurement of plasma power in atmospheric pressure DBD plasma reactors. *Int. J. Appl. Electromagn. Mech.* **2012**, *39*, 81–87. [[CrossRef](#)]
63. Abbasi Khalaki, M.; Ghorbani, A.; Dadjou, F. Influence of Nano-Priming on Festuca ovina Seed Germination and Early Seedling Traits under Drought Stress, in Laboratory Condition. *Ecopersia* **2019**, *7*, 133–139.
64. Karakas, E.; Akman, M.A.; Laroussi, M. The evolution of atmospheric-pressure low-temperature plasma jets: Jet current measurements. *Plasma Sources Sci. Technol.* **2012**, *21*, 034016. [[CrossRef](#)]
65. Tu, X.; Verheyde, B.; Corthals, S.; Paulussen, S.; Sels, B.F. Effect of packing solid material on characteristics of helium dielectric barrier discharge at atmospheric pressure. *Phys. Plasmas* **2011**, *18*, 1–5.
66. Martens, T.; Bogaerts, A.; Brok, W.J.M.; Van Dijk, J. The influence of impurities on the performance of the dielectric barrier discharge. *Appl. Phys. Lett.* **2010**, *96*, 21–24. [[CrossRef](#)]
67. Kostov, K.G.; Borges, A.C.; Koga-Ito, C.Y.; Nishime, T.M.C.; Prysiaznyi, V.; Honda, R.Y. Inactivation of *Candida albicans* by Cold Atmospheric Pressure Plasma Jet. *IEEE Trans. Plasma Sci.* **2015**, *43*, 770–775. [[CrossRef](#)]
68. Schmidt-Bleker, A.; Winter, J.; Bösel, A.; Reuter, S.; Weltmann, K.-D. On the plasma chemistry of a cold atmospheric argon plasma jet with shielding gas device. *Plasma Sources Sci. Technol.* **2016**, *25*, 015005.
69. Kostov, K.G.; Nishime, T.M.C.; Hein, L.R.O.; Toth, A. Study of polypropylene surface modification by air dielectric barrier discharge operated at two different frequencies. *Surf. Coat. Technol.* **2013**, *234*, 60–66. [[CrossRef](#)]

70. Los, A.; Ziuzina, D.; Boehm, D.; Cullen, P.J.; Bourke, P. Investigation of mechanisms involved in germination enhancement of wheat (*Triticum aestivum*) by cold plasma: Effects on seed surface chemistry and characteristics. *Plasma Process. Polym.* **2019**, *16*, 1800148. [[CrossRef](#)]
71. Dobrin, D.; Magureanu, M.; Mandache, N.B.; Ionita, M.D. The effect of non-thermal plasma treatment on wheat germination and early growth. *Innov. Food Sci. Emerg. Technol.* **2015**, *29*, 255–260. [[CrossRef](#)]
72. Iranbakhsh, A.; Ghoranneviss, M.; Oraghi Ardebili, Z.; Oraghi Ardebili, N.; Hesami Tackallou, S.; Nikmaram, H. Non-thermal plasma modified growth and physiology in *Triticum aestivum* via generated signaling molecules and UV radiation. *Biol. Plant.* **2017**, *61*, 702–708. [[CrossRef](#)]
73. Domingos, P.; Prado, A.M.; Wong, A.; Gehring, C.; Feijo, J.A. Nitric oxide: A multitasked signaling gas in plants. *Mol. Plant* **2015**, *8*, 506–520. [[CrossRef](#)]
74. Mittler, R. ROS Are Good. *Trends Plant Sci.* **2017**, *22*, 11–19. [[CrossRef](#)]
75. Wojtyla, L.; Lechowska, K.; Kubala, S.; Garnczarska, M. Different modes of hydrogen peroxide action during seed germination. *Front. Plant Sci.* **2016**, *7*, 1–16.
76. Barba-Espin, G.; Diaz-Vivancos, P.; Clemente-Moreno, M.J.; Albacete, A.; Faize, L.; Faize, M.; Pérez-Alfocea, F.; Hernández, J.A. Interaction between hydrogen peroxide and plant hormones during germination and the early growth of pea seedlings. *Plant Cell Environ.* **2010**, *33*, 981–994.
77. Sasaki, K.; Kishitani, S.; Abe, F.; Sato, T. Promotion of seedling growth of seeds of rice (*Oryza sativa* L. cv. Hitomebore) by treatment with H₂O₂ before sowing. *Plant Prod. Sci.* **2005**, *8*, 509–514. [[CrossRef](#)]
78. Jablonowski, H.; von Woedtke, T. Research on plasma medicine-relevant plasma-liquid interaction: What happened in the past five years? *Clin. Plasma Med.* **2015**, *3*, 42–52. [[CrossRef](#)]



© 2020 by the authors. Licensee MDPI, Basel, Switzerland. This article is an open access article distributed under the terms and conditions of the Creative Commons Attribution (CC BY) license (<http://creativecommons.org/licenses/by/4.0/>).